International Journal of Engineering Science 122 (2018) 1–13

Contents lists available at ScienceDirect

International Journal of Engineering Science

journal homepage: www.elsevier.com/locate/ijengsci

Connections between anisotropic tensors of thermal conductivity and thermal expansion coefficients

Aref Mazloum, Igor Sevostianov*

Department of Mechanical and Aerospace Engineering, New Mexico State University, Las Cruces, NM 88003, United States

ARTICLE INFO

Article history:
Received 21 September 2017
Accepted 18 October 2017

Keywords:
Thermal conductivity
Thermal expansion coefficient
Cross-property connection
Anisotropy
Copper-graphite composite

ABSTRACT

In this paper we derive connections between anisotropic tensors of thermal conductivity and thermal expansion coefficients of a two-phase composite and illustrate it by example of copper containing preferentially oriented graphite flakes. We model the said anisotropic tensors accounting for orientation distribution of the inhomogeneities and derive the cross-property connection by eliminating the microstructural parameters. The model is verified by comparison with the experimental data of Boden (2015) and Firkowska et al. (2015).

1. Introduction

Thermal properties of heterogeneous materials have been studied since XIX century. Comprehensive literature reviews were given by Markov (2000) (on thermal conductivity) and Sevostianov (2012) (on thermal expansion coefficients). In the present work we derive the connection between anisotropic thermal conductivities and thermal expansion coefficients accounting for information on the orientation distribution of the inhomogeneities (that can be obtained, for example, by the implementation of Raman spectroscopy data into micromechanical homogenization models). To the best of our knowledge, the earliest attempts to use analytical approaches accounting for inhomogeneities orientation have been done by Chou and Nomura (1981) and Takao, Chou, and Taya (1982), who considered randomly oriented fibers. Later, Benveniste (1987) used this approach and implemented it in Mori–Tanaka scheme. Similar approach has been developed by Ferrari and Johnson (1989) and Ferrari and Marzari (1992).

To account for orientation distribution intermediates between fully random and perfectly aligned inhomogeneities, various orientation distribution functions have been introduced. Lu and Liaw (1995) proposed to use the combination of Gaussian and trigonometric distributions with respect to the Euler angles: ϕ, θ, and φ:

$$P(\phi,\ \theta,\ \varphi) = P(\phi)P(\theta)P(\varphi) \quad (0 \le \phi,\ \theta,\ \varphi \le \pi) \tag{1.1}$$

where

$$P(\phi) = \frac{2+\cos(2\phi)}{2\pi}, \quad P(\theta) = \sqrt{\frac{2}{\pi}}\exp\left(\frac{-(\theta-\pi/2)^2}{2}\right),$$

* Corresponding author.
E-mail address: igor@nmsu.edu (I. Sevostianov).

https://doi.org/10.1016/j.ijengsci.2017.10.001
0020-7225/

$$P(\varphi) = \sqrt{\frac{2}{\pi}} \exp\left(\frac{-(\varphi - \pi/2)^2}{2}\right) \tag{1.2}$$

To evaluate the themal conductivity of a transversly isotropic material, Chen and Wang (1996) proposed to use the following orientation distribution function

$$P(\theta) = 1 - \exp(\lambda\theta) \tag{1.3}$$

Pettermann, Böhm, and Rammerstorfer (1997) used exponential orientation distribution function

$$P(\theta) = \exp\left(-\theta^2/2\lambda^2\right) \tag{1.4}$$

and implemented it in Mori–Tanaka scheme. Sevostianov and Kachanov (1999) described transversly isotropic orientation distribution of cracks using the folloing function:

$$P_\lambda(\varphi) = \frac{1}{2\pi}\left[\left(\lambda^2 + 1\right) e^{-\lambda\varphi} + \lambda e^{-\lambda\pi/2}\right] \tag{1.5}$$

Note that the orientation distribution as well as the shape of the inhomogeneities affect both thermal conductivity and thermal expansion coefficient in a similar manner and, therefore, they can be linked to each other (as discussed by Sevostianov & Kachanov, 2009). Anisimova, Knyazeva, and Sevostianov (2016) derived the cross-property connection for aluminum containing diamond particles and verified it experimentally. Kováčik, Emmer, and Bielek (2016) reported experimental data on the connection between isotropic thermal, electric, and mechanical properties of copper-graphite composites. Mazloum, Kováčik, Emmer, and Sevostianov (2016) developed a micromechanical model for these observations. In all these papers the overall properties of the composites have been isotropic. In the present paper, we focus on the overall transverse isotropy of a material containing transversely-isotropic graphite flakes that have a certain preferential orientation varying from perfect alignment to fully random distribution. The theoretical results are compared with experimental data of Boden (2015) and Firkowska et al. (2015).

2. Background material: property contribution tensors

Property contribution tensors are introduced to describe the input from an inhomogeneity to the overall property of interest. In the context of elastic properties, compliance contribution tensor $\boldsymbol{H}$ has been first introduced by Horii and Nemat-Nasser (1983) for ellipsoidal pores and cracks. Sevostianov and Kachanov (2002) proposed to use conductivity and resistivity contribution tensors $\boldsymbol{K}$ and $\boldsymbol{R}$ to describe overall thermal or electric conductivities of heterogeneous materials. Below, we brieflydescribe their approach. Assuming a linear dependence between the temperature gradient ∇T and the remote heat flux $\boldsymbol{q}^0$, the extra temperature gradient required to keep the same heat flux over reference volume V in the presence of the inhomogeneity of volume $V_1 << V$ is

$$\Delta(\nabla T) = \frac{V_1}{V}\boldsymbol{R}\cdot\boldsymbol{q}^0 \tag{2.1}$$

where $\boldsymbol{R}$ is the inhomogeneity's resistivity contribution tensor (a symmetric second-rank tensor). A dual conductivity contribution tensor can be introduced in a similar manner:

$$\Delta\boldsymbol{q} = \frac{V_1}{V}\boldsymbol{K}\cdot(\nabla T)^0 \tag{2.2}$$

where $(\nabla T)^0$is the remotely applied temperature gradient.

For an isotropic matrix of conductivity k_0, the resistivity and conductivity contribution tensors are interrelated by

$$\boldsymbol{K} = -k_0^2\boldsymbol{R} \tag{2.3}$$

For a spheroidal transversely-isotropic inhomogeneity (axes of its geometrical and material symmetries coincide) embedded in an isotropic matrix, the resistivity and conductivity contribution tensors have the following form (Sevostianov & Giraud, 2013):

$$\boldsymbol{R} = -\frac{1}{k_0^2}\boldsymbol{K} = \frac{1}{k_0}\left[A_1(\boldsymbol{I} - \boldsymbol{nn}) + A_2\boldsymbol{nn}\right] \tag{2.4}$$

where dimensionless parameters A_1 and A_2 are expressed as:

$$A_1 = \frac{1 - k_{11}^1/k_0}{1 - \left(1 - k_{11}^1/k_0\right)f_0}, \quad A_2 = \frac{1 - k_{33}^1/k_0}{k_{33}^1/k_0 + 2\left(1 - k_{33}^1/k_0\right)f_0} \tag{2.5}$$

and shape factor f_0 is given by formula (A.10) in the Appendix.

The thermal expansion contribution tensor of an inhomogeneity A_{ij} has been introduced by Sevostianov (2012) as an extra strain over volume V produced by prescribed temperature change ΔT due to the presence of the inhomogeneity:

$$\varepsilon_{ij} = \alpha_{ij}^0\Delta T + \frac{V_1}{V}\mathrm{A}_{ij}\Delta T \tag{2.6}$$

This additional strain can be expressed as follows (Sevostianov, 2012):

$$\Delta\varepsilon_{ij} = \mathrm{A}_{ij}\Delta T = H_{ijkl}\left(S^1_{klmn} - S^0_{klmn}\right)^{-1}\left(\alpha^1_{mn} - \alpha^0_{mn}\right)\,\Delta T \tag{2.7}$$

where S^1_{klmn} and S^0_{klmn} are respectivly compliances of the inhomogeneity and the matrix and H_{ijkl} is the compliance contribution tensor of the inhomogeneity (see the Appendix). For transversely isotropic spheroidal inhomogeneities, tensor $\boldsymbol{A}$ has the following form (Mazloum et al., 2016):

$$\mathbf{A} = \alpha_0[M_1\boldsymbol{I} + (M_2 - M_1)\boldsymbol{nn}] \tag{2.8}$$

where

$$M_1 = \frac{w_2\left(\alpha^1_{11} - \alpha_0\right) - w_3\left(\alpha^1_{33} - \alpha_0\right)}{2\alpha_0(w_1w_2 - w_3w_4)}; \quad M_2 = \frac{w_1\left(\alpha^1_{33} - \alpha_0\right) - w_4\left(\alpha^1_{11} - \alpha_0\right)}{\alpha_0(w_1w_2 - w_3w_4)} \tag{2.9}$$

and expressions for factors w_i are given in the Appendix by formula (A.13).

3. Calculations of the effective thermal properties of anisotropic composites

In the case of multiple inhomogeneities, extra temperature gradient due to kth inhomogeneity required to keep the same remote heat flux is $\Delta(\nabla T^{(k)}) = \frac{V_k}{V}\boldsymbol{R}^{(k)}\cdot\boldsymbol{q}^0$ so that the total extra resistivity due to all the inhomogeneities is given by

$$\Delta\,\boldsymbol{r} = \frac{1}{V}\sum V_k\boldsymbol{R}^{(k)} \tag{3.1}$$

Strictly speaking, $\boldsymbol{R}^{(k)}$ tensors in (3.1) are affected by the interaction between inhomogeneities. However, as discussed by Kachanov and Sevostianov (2005), it is much more practical to take $\boldsymbol{R}^{(k)}$ tensors in the non-interaction approximation and use one of the homogenization schemes to describe the interaction. Such schemes place the non-interacting inhomogeneities into some sort of effective environment (effective matrix or effective field) and can be formulated in terms of $\boldsymbol{R}$-tensors for non-interacting inhomogeneities. Formula (3.1) highlights the fundamental importance of the property contribution tensors: it is *them,* which have to be summed up in the context of the effective material properties. The sums

$$\frac{1}{V}\sum V_k\boldsymbol{R}^{(k)} \quad\text{and}\quad \frac{1}{V}\sum V_k\boldsymbol{K}^{(k)} \tag{3.2}$$

properly reflect resistivity/conductivity contributions of individual inhomogeneities into the overall properties.

Similarly, the total extra thermal expansion is given by

$$\Delta\,\boldsymbol{\alpha} = \frac{1}{V}\sum V_k\boldsymbol{A}^{(k)} \tag{3.3}$$

Each of the sums in (3.2) and (3.3) constitutes the *general microstructural parameters* in the context of the effective thermal properties. If all the inhomogeneities are of the same shape and size, summations in (3.1)–(3.3) may be replaced by integrations over orientations of the inhomogeneities.

3.1. Non-interaction approximation (NIA)

When the interaction between individual inhomogeneities is disregarded, every inhomogeneity can be considered as an isolated one. Then, replacing summation by integration over orientations, as discussed above, yields

$$\nabla T = \frac{1}{k_0}\boldsymbol{q}^0 + c\cdot\langle\boldsymbol{R}\rangle\cdot\boldsymbol{q}^0 \tag{3.4}$$

where c is the volume fraction of the inhomogeneities,

$$\langle\boldsymbol{R}\rangle = \frac{1}{k_0}\left[A_1\boldsymbol{I} + (A_2 - A_1)\langle\boldsymbol{nn}\rangle\right] \tag{3.5}$$

and $\boldsymbol{n}$ is a unit vector along the ith spheroid's symmetry axis that is expressed in polar coordinates $0 \le \phi \le \pi/2$ and $0 \le \theta \le 2\pi$ (Fig. 1) as follows

$$\boldsymbol{n}(\varphi,\theta) = \cos\theta\sin\varphi\,\boldsymbol{e_1} + \sin\theta\sin\varphi\,\boldsymbol{e}_2 + \cos\varphi\,\boldsymbol{e}_3 \tag{3.6}$$

The average tensor $\langle\boldsymbol{nn}\rangle$ can be calculated using the orientaintion distribution function as follows:

$$\langle\boldsymbol{nn}\rangle = \int_0^{2\pi}\left[\int_0^{\pi/2} P(\varphi)\cdot\boldsymbol{nn}\cdot\sin\varphi\cdot d\varphi\right]\cdot d\theta \tag{3.7}$$

The exact form of function $P(\varphi)$ does not produce a major effect on the overall properties (Kachanov et al., 1994). In the present paper we use the orientation distribution function introduced by Sevostianov and Kachanov (1999) (to simplify the process of comparison with the experimental data of Boden (2015)):

$$P_\mu(\varphi) = \frac{1}{2\pi}\left[\left(\mu^2 + 1\right)e^{-\mu\varphi} + \mu e^{-\mu\pi/2}\right] \tag{3.8}$$

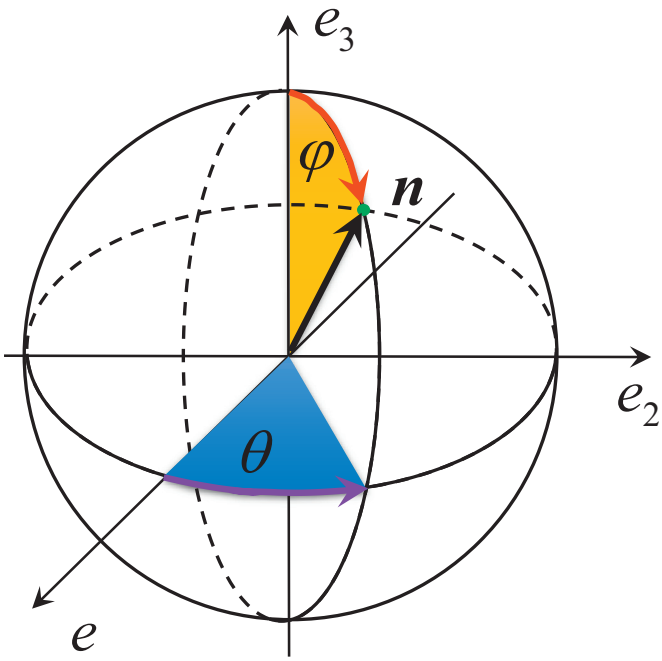

Fig. 1. Representation of vector $\boldsymbol{n}$ in the spherical coordinates used in Eq. (3.6).

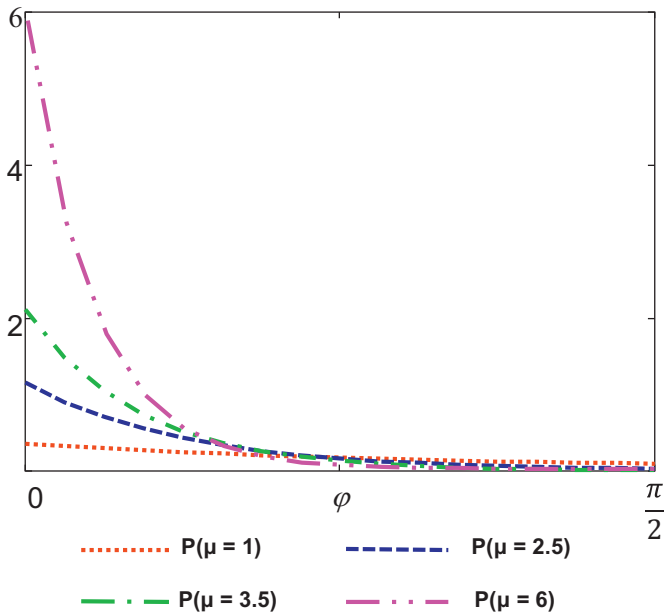

Fig. 2. Representation of scattering parameter μ.

where μ represents the scattering parameter (see Fig. 2). It plays the following role: if μ approaches zero, then the graphite flakes tend to be randomly oriented. As μ increases, the scatter decreases and when μ is about 3 the preferential orientation of the inhomogeneities can be identified. As μ approaches infinty the graphite flakes are pefectly alligned (actually, already at $\mu = 6$, the orientation of the flakes is very close to the prefect alignmnet, as shown in Fig. 2). The average tensors $\langle \boldsymbol{nn} \rangle$ can be represented in the following form:

$$\langle \boldsymbol{nn} \rangle = \beta_1 (\boldsymbol{e_1 e_1} + \boldsymbol{e_2 e_2}) + \beta_3 (\boldsymbol{e_3 e_3}) = \beta_1 \boldsymbol{I} + (\beta_3 - \beta_1) \boldsymbol{e_3 e_3} \tag{3.9}$$

where

$$\beta_1 = \pi \cdot \int_0^{\pi/2} P(\varphi) \cdot \sin^3\varphi \cdot d\varphi = \frac{18 - \mu\left(3+\mu^2\right) e^{\frac{\mu\pi}{2}}}{6\left(9+\mu^2\right)} \tag{3.10}$$

$$\beta_3 = 2\pi \cdot \int_0^{\pi/2} P(\varphi) \cdot \cos^2\varphi \cdot \sin\varphi \cdot d\varphi = \frac{\left(3+\mu^2\right) e^{\frac{\mu\pi}{2}}\left(\mu + 3e^{\frac{\mu\pi}{2}}\right)}{3\left(9+\mu^2\right)} \tag{3.11}$$

Then, the effective resistivity in the framework of non-interaction approximation has the following form:

$$\left\langle \boldsymbol{R}^{\mathbf{NI}} \right\rangle = \frac{c}{k_0}[(A_1 + (A_2 - A_1)\beta_1)\boldsymbol{I} + (A_2 - A_1)(\beta_3 - \beta_1)\boldsymbol{e_3}\boldsymbol{e_3}] \equiv \frac{c}{k_0}\boldsymbol{\eta} \tag{3.12}$$

where A_1 and A_2 are given by (2.5). Then, the effective conductivities in the plane of isotropy and transverse direction are

$$k_{11}^{eff} = \frac{k_0}{1 + c\eta_{11}}; \quad k_{33}^{eff} = \frac{k_0}{1 + c\eta_{33}} \tag{3.13}$$

In the same manner, the average strain produced by temperature change in the volume containing multiple homogeneities is

$$\boldsymbol{\varepsilon} = \alpha_0 T[\boldsymbol{I} + c \cdot \langle \mathbf{A} \rangle] \tag{3.14}$$

Implementation of the expressions (2.8) and (3.7) yields

$$\begin{aligned} \boldsymbol{\varepsilon} &= \alpha_0[\boldsymbol{I} + c(M_1 + (M_2 - M_1)\beta_1)\boldsymbol{I} + c(M_2 - M_1)(\beta_3 - \beta_1)\boldsymbol{e_3}\boldsymbol{e_3}]\Delta T \\ &\equiv \alpha_0[\boldsymbol{I} + c\boldsymbol{\zeta}]\Delta T \end{aligned} \tag{3.15}$$

where M_1 and M_2 are given by (2.9). Then, the effective thermal expansion coefficients in the plane of isotropy and transverse direction are expressed as follows:

$$\alpha_{11}^{eff} = \alpha_0[1 + c \cdot \boldsymbol{\zeta}_{11}], \quad \alpha_{33}^{eff} = \alpha_0[1 + c \cdot \boldsymbol{\zeta}_{33}] \tag{3.16}$$

Non-interaction approximation serves as the basic building block for various micromechanical homogenization schemes. Below we illustrate it on an example of Maxwell homogenization scheme.

3.2. Maxwell's scheme

In his original work, Maxwell (1873) considered a large sphere with the unknown effective conductivity k_{eff} embedded in the background material of conductivity k_0 and containing non-interacting small spheres of conductivity k_1 and volume fraction c. He calculated the far-field asymptotics of the perturbation of the externally applied electric field in two different ways: (1) as a sum of far-fields generated by the small spheres, and (2) as the far-field generated by the large sphere. Equating the two yields the effective conductivity k_{eff}. Sevostianov and Giraud (2013) reformulated Maxwell's scheme in terms of property contribution tensors for the general case of anisotropic materials. It can be written as follows:

$$\frac{1}{r^0}\boldsymbol{r}^{eff} = \boldsymbol{I} + \left[\frac{1}{c}\boldsymbol{\eta}^{-1} - r^0\,\mathbf{Q}^{\Omega}\right]^{-1} = \boldsymbol{I} + c\,\boldsymbol{\eta}\left[\boldsymbol{I} - c\,r^0\,\boldsymbol{\eta}\cdot\mathbf{Q}^{\Omega}\right]^{-1} \tag{3.17}$$

where $\mathbf{Q}^{\Omega}$ is 2nd rank Hill's tensor (Hill's tensor for conductivity problem) calculated for the effective domain Ω (its components strongly depend on the shape of Ω as shown in the Appendix—see formula (A.12)). Sevostianov (2014) suggested a method to evaluate the shape of Ω (numerically verified by Kushch and Sevostianov, (2016)). In our case, Ω is a spheroid with the aspect ratio $\Gamma = \eta_{11}/\eta_{33}$. After some algebra, the effective thermal conductivities in the plane of isotropy and in the transverse direction can be respectively formulated as follows:

$$k_{11}^{eff} = k_0\frac{1 - c\,\Psi_{\mathbf{11}}}{1 + c\,(\eta_{\mathbf{11}} - \Psi_{\mathbf{11}})}\cdot; \quad k_{33}^{eff} = k_0\frac{1 - c\,\Psi_{33}}{1 + c\,(\eta_{33} - \Psi_{33})}\cdot \tag{3.18}$$

where $\boldsymbol{\Psi} = r_0\boldsymbol{\eta}\cdot\mathbf{Q}^{\Omega}$.

Tensor of the effective thermal expansion coefficient can be calculated using the approach introduced by Sevostianov (2012). In the case of interest, the thermal expansion coefficients tensor can be expressed as follows:

$$\frac{1}{\alpha_0}\boldsymbol{\alpha}^{eff} = \boldsymbol{I} + \left[\frac{1}{c}\,\boldsymbol{\zeta}^{-1} - \tilde{\mathbf{Q}}^{\Omega}\right]^{-1} = \boldsymbol{I} + c\boldsymbol{\zeta}\cdot\left[\boldsymbol{I} - \frac{c}{\alpha_0}\boldsymbol{\zeta}\,\tilde{\mathbf{Q}}^{\Omega}\right]^{-1} \tag{3.19}$$

where the second rank tensor $\tilde{\mathbf{Q}}^{\Omega}$ is expressed in terms of the fourth-rank Hill's tensor for elasticity problem $\hat{\mathbf{Q}}^{\Omega}$ and differences in thermal expansion $(\boldsymbol{\alpha}_1 - \boldsymbol{\alpha}_0)$ and elastic compliances $(\boldsymbol{S}_1 - \boldsymbol{S}_0)$ of two materials:

$$\tilde{\mathbf{Q}}^{\Omega} = (\boldsymbol{\alpha}_1 - \boldsymbol{\alpha}_0)^{-1} : (\boldsymbol{S}_1 - \boldsymbol{S}_0) : \hat{\mathbf{Q}}^{\Omega} \tag{3.20}$$

Components of tensor $\hat{\boldsymbol{Q}}^{\Omega}$ are given in the Appendix by (A.9). Generally, the shape of Ω depends on the problem of interest (it is one of the main disadvantages of the Maxwell scheme). Due to that, the aspect ratio in the problem of thermal expansion has to be calculated from the compliance contribution tensors. The difference, however, is mild and we used $\Gamma = \eta_{11}/\eta_{33}$ for thermal expansion problem as well. Predictions of the NIA and Maxwell homogenization scheme will be compared with the experimental data in Section 5.

4. Cross-property connections

Cross-property connections link changes in different physical properties of materials due to the presence of inhomogeneities, or, more generally—due to development of microstructure. The existance of the relations of this kind is based on the possibility to express two different properties in terms of the same microstructural parameter. The detailed review of the history of cross-property connections is given by Sevostianov and Kachanov (2009). Mazloum et al. (2016) established cross-property connection between thermal expansion coefficient and thermal and electrical conductivities of two-phase macroscopically isotropic composites. In the present work, we use the results presented in the previous section to establish connections between *anisotropic* tensors of thermal conductivity and thermal expansion coefficients.

We start from rewriting the expressions for overall thermal properties obtained in the previous Section in somewhat different form. In the context of non-interaction approximation, the overall thermal resistivity tensor can be written as

$$\boldsymbol{r}^{eff} = r_0\boldsymbol{I} + c\langle\boldsymbol{R}\rangle = r_0\boldsymbol{I} + c\frac{1}{k_0}\left[A_1\boldsymbol{I} + (A_2 - A_1)\langle\boldsymbol{nn}\rangle\right] \tag{4.1}$$

where coefficients A_1 and A_2 are given by (2.5). The thermal expansion coefficients tensor is:

$$\boldsymbol{\alpha}^{eff} = \alpha_0\boldsymbol{I} + c\langle\mathbf{A}\rangle = \alpha_0\boldsymbol{I} + c\alpha_0\left[M_1\boldsymbol{I} + (M_2 - M_1)\langle\boldsymbol{nn}\rangle\right] \tag{4.2}$$

with coefficients M_1 and M_2 given by (2.9). Factors A_i and M_i depend on the material properties and shapes of the inhomogeneities. If inhomogeneities are spheroids and their aspect ratios are not correlated with either orientations of the inhomogeneities or their volumes, coefficients A_i and M_i can be replaced by their averages and taken out of the summation. Then tensors $\boldsymbol{r}^{eff}$ and $\boldsymbol{\alpha}^{eff}$ are expressed in terms of the same second rank symmetric tensor

$$\boldsymbol{\omega} = \frac{1}{V}\sum_k V^{(k)}(\boldsymbol{nn})^{(k)} = c\langle\boldsymbol{nn}\rangle = c[\beta_1\boldsymbol{I} + (\beta_3 - \beta_1)\boldsymbol{e_3}\boldsymbol{e_3}] \tag{4.3}$$

(note that $tr(\boldsymbol{\omega})$ is the volume fraction of the inhomogeneities c) as follows:

$$\boldsymbol{r}^{eff} = r_0\boldsymbol{I} + r_0\ (c\ a_1\boldsymbol{I} + (a_2 - a_1)\ \boldsymbol{\omega}) \tag{4.4}$$

$$\boldsymbol{\alpha}^{eff} = \alpha_0\boldsymbol{I} + \alpha_0\ (c\ m_1\boldsymbol{I} + (m_2 - m_1)\ \boldsymbol{\omega}) \tag{4.5}$$

Coefficients a_i and m_i are average shape factors for the thermal conductivity and coefficient of thermal expansion (CTE) problems:

$$a_i = \int_0^\infty A_i(\gamma)\,p(\gamma)\,d\gamma \quad m_i = \int_0^\infty M_i(\gamma)\,p(\gamma)\,d\gamma \tag{4.6}$$

where $p(\gamma)$ is the shape distribution density.

To derive cross-property connection between the tensors of the overall thermal resistivity and thermal expansion, it is more convenient to represent the tensors as the sums of their volumetric and deviatoric parts. Then

$$\frac{1}{r_0}\boldsymbol{r}^{eff} - \boldsymbol{I} = c\boldsymbol{\eta} = \frac{c}{3}(a_2 + 2a_1)\,\boldsymbol{I} + (a_2 - a_1)\boldsymbol{\omega}' \tag{4.7}$$

$$\frac{1}{\alpha_0}\alpha^{eff} - \mathbf{I} = c\zeta = \frac{c}{3}(m_2 + 2m_1)\,\mathbf{I} + (m_2 - m_1)\omega' \tag{4.8}$$

Where prime indicates the deviatoric parts. Eliminating now c and $\boldsymbol{\omega}'$ we get explicit cross-property connection between thermal and electrical properties.:

$$\frac{1}{\alpha_0}\alpha_{ij}^{eff} - \delta_{ij} = \frac{2m_1 + m_2}{2a_1 + a_2}\left(\frac{1}{3r_0}r_{kk}^{eff} - 1\right)\delta_{ij} + \frac{m_2 - m_1}{a_2 - a_1}\frac{1}{r_0}r_{ij}^{\prime eff} \tag{4.9}$$

where $r_{ij}^{\prime eff}$ is deviatoric part of tensor r_{ij}^{eff}. This connection is exact in the framework of non-interaction approximation. In general $\frac{2m_1+m_2}{2a_1+a_2}$ and $\frac{m_2-m_1}{a_2-a_1}$ are shape dependent.

Expressions (3.17) and (3.19) yield the connection between effective thermal expansion and thermal resistivity tensors in the framework of Maxwell scheme. Indeed, introducing notations

$$\tilde{r}_{11} \equiv \frac{r_{11}^{eff} - r_0}{r_0\left[1 + Q_{11}^{\Omega}\left(r_{11}^{eff} - r_0\right)\right]}; \quad 1 \to 2 \to 3 \tag{4.10}$$

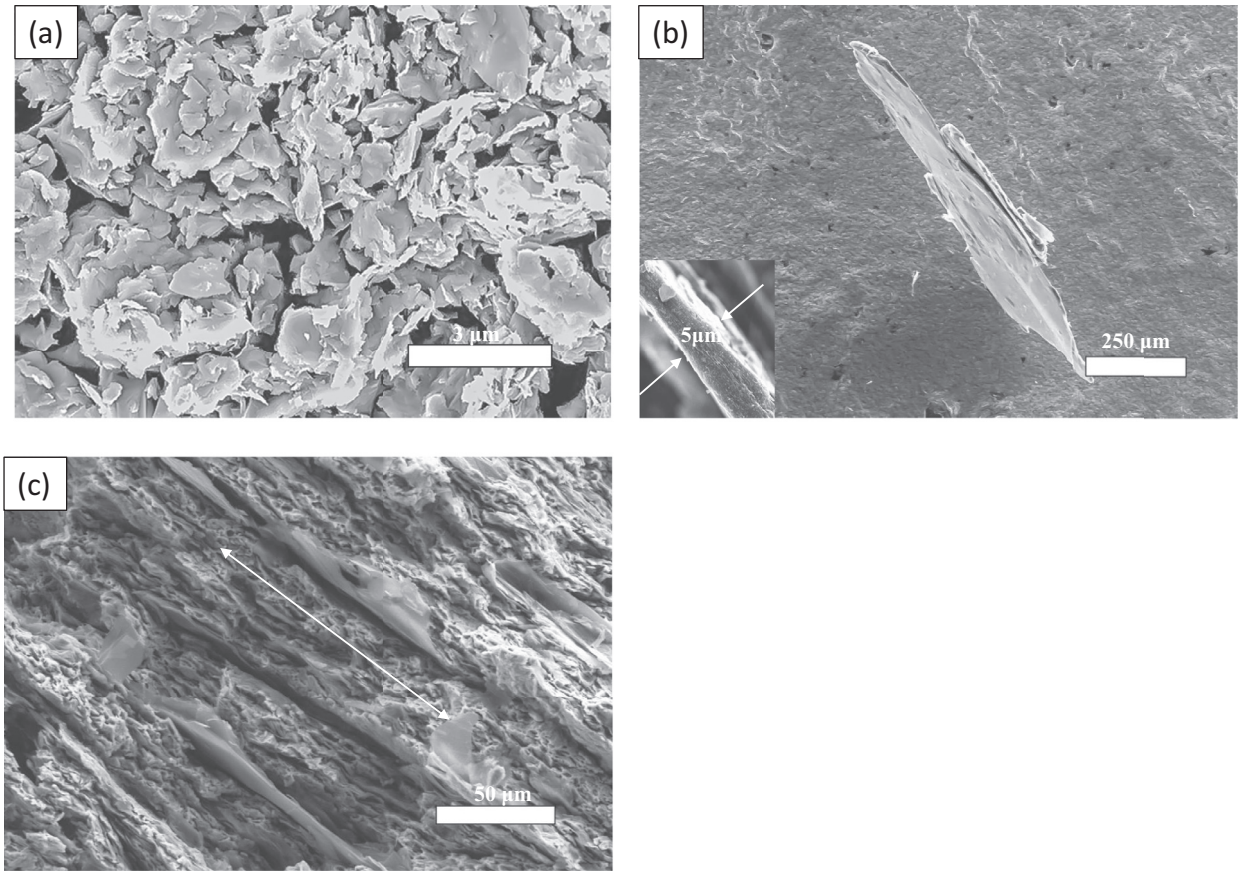

Fig. 3. (a) SEM image of copper powder, (b) SEM image of a graphite flake and its thickness; (c) SEM image of Cu-graphite composite at a specimen's fractural cross section with the preferable direction of alignment (Boden, 2015).

we can express

$$c\eta_{ij} = \tilde{r}_{ij}, \tag{4.11}$$

or, representing both sides in terms of the sums of volumetric and deviatoric parts,

$$\frac{c}{3}(a_2 + 2a_1)\,\delta_{ij} + (a_2 - a_1)\boldsymbol{\omega}'_{ij} = \frac{1}{3}\tilde{r}_{kk}\delta_{ij} + \tilde{r}'_{ij} \tag{4.12}$$

This expression, together with (3.19) yields the desired cross-property connection:

$$\frac{1}{\alpha_0}\boldsymbol{\alpha}^{eff} - \boldsymbol{I} = \boldsymbol{\Lambda} \cdot \left[\boldsymbol{I} - \alpha_0 \boldsymbol{\Lambda} \cdot \tilde{\boldsymbol{Q}}^{\Omega}\right]^{-1} \tag{4.13}$$

where

$$\boldsymbol{\Lambda} = \frac{(m_2 + 2m_1)}{3(a_2 + 2a_1)} tr(\tilde{\boldsymbol{r}})\boldsymbol{I} + \frac{(m_2 - m_1)}{(a_2 - a_1)}\tilde{\boldsymbol{r}}' \tag{4.14}$$

and $tr(\tilde{\boldsymbol{r}})$ is trace of dimensionless tensor $\tilde{\boldsymbol{r}}$ introduced by (4.10) and $\tilde{\boldsymbol{r}}'$ is its deviatoric part.

5. Copper containing graphite flakes

In this section we validate our approach using experimental data of Boden (2015) and Firkowska et al. (2015) on copper-graphite composites that possess thermal conductivity up to 1.4 times higher than those of copper and low thermal expansion (comparable with the thermal expansion of semiconductors, Boden, 2015; Tong, 2011). In the work of Boden (2015) and Firkowska et al. (2015), copper-graphite composites with volume fraction of graphite flakes varying from 0.08 to 0.5 were prepared using high energy ball milling to mix the copper powder with an approximate particle size 3 µm (Fig. 3a) with

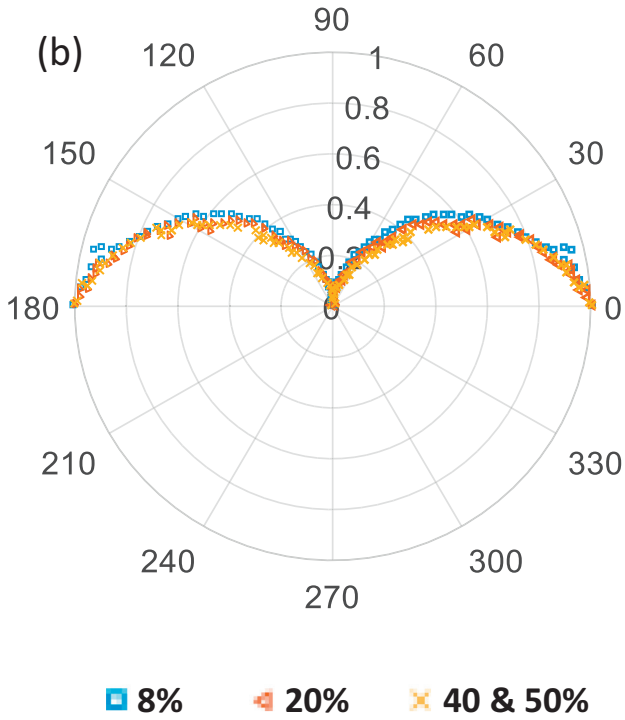

Fig. 4. Polar plot of the G peak intensity of composites containing different volume fractionsa of graphite flakes over the polarization angle.

Table 1
The values of μ for different grapihite flakes vol.%.

Graphite flakes vol.%	μ
8	2.4
20	2.6
40	2.8
50	2.8

Table 2
Experimentally measured thermal properties of copper- graphite composite in dependence on volume fraction of graphite (c).

Graphite vol.%	Thermal conductivity In isotropy plane	Thermal conductivity in transverse direction	CTE In isotropy plane	CTE in transverse direction	Alignment
C	[W/mK]	[W/mK]	[10^{-6} K^{-1}]	[10^{-6} K^{-1}]	%
0	340	340	17.43	17.44	0
8	300	200	16.59	17.10	54
20	338	143	15.58	16.82	58
40	481	65	14.35	4.93	80
50	504	47	12.11	1.96	80

G300 micro-graphite flakes of an approximate flake lateral length 300μ and 5μ of thickness (Fig. 3b). Consolidation of Cu-graphite composites was obtained by spark plasma sintering. After the specimens were prepared (Fig. 3c), a Raman spectrum was applied and the intensity of G-line was determined according to the angle of polarization due to the orientation of graphite planes of isotropy (see Fig. 4). This dependence was used to calculate the orientation distribution of graphite flakes. The values of the scattering parameter μ for different graphite flakes volume fractions are given in Table 1.

Thermal conductivities have been measured using guarded hot plate method in two directions—parallel to the plane of isotropy (basal plane) and transverse direction. Thermal expansion coefficients have been measured using a dilatometer. All thermal measurements are provided in Table 2. Due to the orientation of the graphite flakes, the carryover effect of its in isotropy plane CTE influenced the entire composite, which made the composites' CTEs in both directions (in isotropy plane and transverse direction) decreasing as the volume fraction of graphite flakes increases (Table 2). Material constants of the

Table 3
Material constants of the constituents.

Constituent	Copper	Graphite
Thermal conductivity[(1)]		
$k_{11} = k_{22}$	340 W/m K	1500 W/m K
k_{33}		15 W/m K
Thermal expansion coefficient[(1)]		
$\alpha_{11} = \alpha_{22}$	17.5×10^{-6} K^{-1}[(1)]	-1.5×10^{-6} K^{-1}[(3)]
α_{33}		28×10^{-6} K^{-1}[(3)]
Modulus of elasticity		
$E_{11} = E_{22}$	124 GPa[(2)]	1109 GPa[(4)]
E_{33}		38.7 GPa[(4)]
Bulk modulus		
K	140 GPa[(2)]	36.4 GPa[(4)]
Shear modulus		
$G_{11} = G_{22}$	44 GPa[(2)]	485 GPa[(4)]
G_{33}		5 GPa[(4)]
Poisson's ratio		
ν_{12}	0.35[(2)]	0.12[(4)]
ν_{13}		0.01[(4)]
Elastic stiffness [(5)]		
C_{1111}	192.47 GPa	920 GPa
C_{1122}	105.7 GPa	33 GPa
C_{1313}	43.17 GPa	2.3 GPa
C_{3333}	192.47 GPa	30 GPa
C_{1133}	105.7 GPa	0 GPa

(1) Boden (2015).
(2) Ledbetter and Naimon (1974).
(3) Nelson and Riley (1945).
(4) Bosak, Krisch, Mohr, Maultzsch, and Thomsen (2007).
(5) Chen (1993).

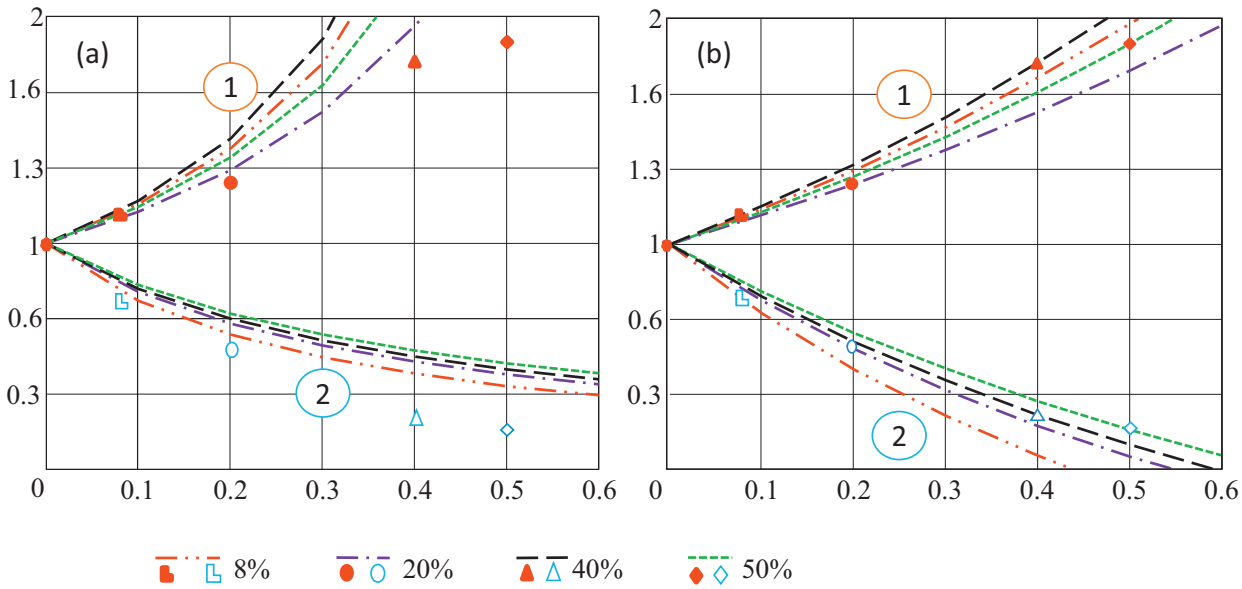

Fig. 5. Comparison of the thermal conductivities calculated by (a) Non-interaction approximation and (b) Maxwell's scheme with the experimental data. Group (1) lines are for thermal conductivities in the plane of isotropy. Group (2) lines are for thermal conductivities in transverse direction.

composite constituents are presented in Table 3. Figs. 5 and 6 illustrate comparisons of the predictions provided by (a) non-interaction approximation (formulas (3.13) and (3.16)) and (b) Maxwell's scheme (formulas (3.18) and (3.19)) with the experimental data of thermal conductivities and thermal expansion coefficients, respectively. For cross-property connection, evaluations of Eqs. (4.9) and (4.13) with experimental data are illustrated in Fig. 7.

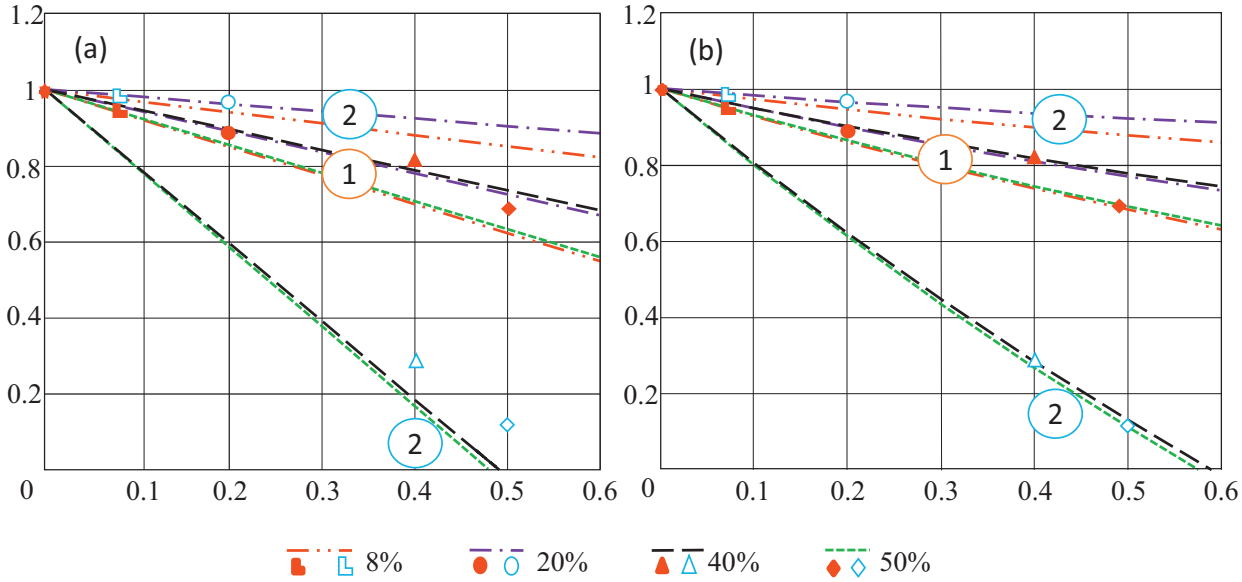

Fig. 6. Comparison of the thermal expansion coefficients calculated by (a) Non-interaction approximation and (b) Maxwell's scheme with the experimental data. Group (1) lines are for CTE in the plane of isotropy. Group (2) lines are for CTE in transverse direction.

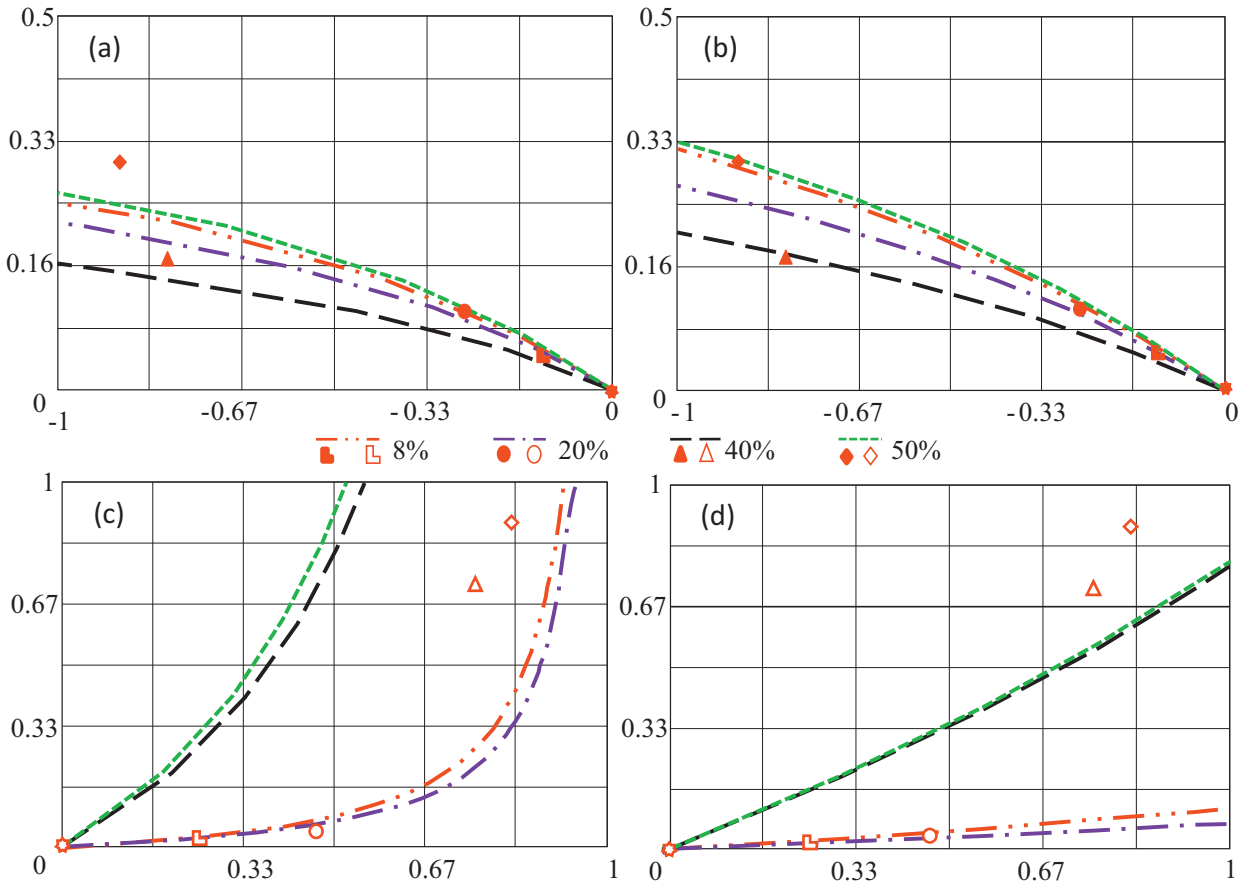

Fig. 7. Comparison of the cross-property connection (4.9) and (4.13) with experimental data (a) Non-interaction approximation, plane of isotropy; (b) Maxwell's scheme, plane of isotropy; (c) Non-interaction approximation, transverse direction; (d) Maxwell's scheme, transverse direction.

6. Concluding remarks

The paper addresses effective thermal properties of anisotropic two-phase materials. We emphasize that the problem of calculation of the anisotropic effective properties of a composite is closely related to the one of quantitative characterization of composite microstructure—identification of microstructural parameters, in its terms the tensors of the thermal conductivity and thermal expansion are to be expressed. These proper microstructural parameters should represent the individual inhomogeneities in accordance with their contributions to the properties (Kachanov & Sevostianov, 2005). We explicitly derived these parameters and expressed effective thermal properties of a composite in their terms.

Our results are given in closed form that explicitly reflects shapes of inhomogeneities and their orientation distribution. They are derived in the non-interaction approximation and in the frameworks of the Maxwell homogenization scheme. It is shown that the Maxwell scheme properly predicts behavior of the heterogeneous material at high limit of the inhomogeneities. We also derived cross-property connections between anisotropic tensors of thermal conductivity and thermal expansion of a two-phase composite. The established cross-property connections are important for various applications such as heat sinks, especially when high conductivity in basal plane direction and low thermal expansion coefficient are the requirements. Note that thermal conductivities and CTEs depend on one another and are governed by the same microstructural parameters. It makes the optimization of these properties only possible through the cross-property connections. We compared our derivation with the experimental data for copper graphite composite obtained by Boden (2015) and Firkowska (2015). The agreement is generally very good.

Acknowledgement

This work was supported by NASA Cooperative Agreement NNX15AL51H (through NM Space Grant Consortium) and grant 14.Z50.31.0036 awarded by Department of Education and Science of the Russian Federation to R. E. Alexeev Nizhny Novgorod Technical University.

Appendix. Tensor basis in the space of transversely isotropic fourth rank tensors. Representation of certain transversely isotropic tensors in terms of the tensor basis

The operations of analytic inversion and multiplication of fourth rank tensors are conveniently done in terms of special tensor bases that are formed by combinations of unit tensor δ_{ij} and one or two orthogonal unit vectors (Kunin, 1983; Kanaun & Levin, 2007). In the case of the transversely isotropic elastic symmetry, the following basis is most convenient (it differs slightly from the one used by Kanaun and Levin (2007)):

$$\begin{aligned} &T^{(1)}_{ijkl} = \theta_{ij}\theta_{kl}, \quad T^{(2)}_{ijkl} = \left(\theta_{ik}\theta_{lj} + \theta_{il}\theta_{kj} - \theta_{ij}\theta_{kl}\right)/2, \quad T^{(3)}_{ijkl} = \theta_{ij}m_k m_l, \quad T^{(4)}_{ijkl} = m_i m_j \theta_{kl} \\ &T^{(5)}_{ijkl} = \left(\theta_{ik}m_l m_j + \theta_{il}m_k m_j + \theta_{jk}m_l m_i + \theta_{jl}m_k m_i\right)/4, \quad T^{(6)}_{ijkl} = m_i m_j m_k m_l \end{aligned} \tag{A.1}$$

where $\theta_{ij} = \delta_{ij} - m_i m_j$ and $\boldsymbol{m} = m_1\boldsymbol{e}_1 + m_2\boldsymbol{e}_2 + m_3\boldsymbol{e}_3$ is a unit vector along the axis of transverse symmetry.

These tensors form the closed algebra with respect to the operation of (non-commutative) multiplication (contraction over two indices):

$$\left(\boldsymbol{T}^{(\alpha)}:\boldsymbol{T}^{(\beta)}\right)_{ijkl} \equiv T^{(\alpha)}_{ijpq}T^{(\beta)}_{pqkl} \tag{A.2}$$

The inverse of any fourth rank tensor $\boldsymbol{X}$, as well as the product $\boldsymbol{X}:\boldsymbol{Y}$ of two such tensors are readily found in the closed form, as soon as the representation in the basis

$$\boldsymbol{X} = \sum_{k=1}^{6} X_k \boldsymbol{T}^{(k)}, \quad \boldsymbol{Y} = \sum_{k=1}^{6} Y_k \boldsymbol{T}^{(k)} \tag{A.3}$$

are established. Indeed:

a) Inverse tensor $\boldsymbol{X}^{-1}$ defined by $X^{-1}_{ijmn}X_{mnkl} = (X_{ijmn}X^{-1}_{mnkl}) = J_{ijkl}$ is given by

$$\boldsymbol{X}^{-1} = \frac{X_6}{2\Delta}\boldsymbol{T}^{(1)} + \frac{1}{X_2}\boldsymbol{T}^{(2)} - \frac{X_3}{\Delta}\boldsymbol{T}^{(3)} - \frac{X_4}{\Delta}\boldsymbol{T}^{(4)} + \frac{4}{X_5}\boldsymbol{T}^{(5)} + \frac{2X_1}{\Delta}\boldsymbol{T}^{(6)} \tag{A.4}$$

where $\Delta = 2(X_1X_6 - X_3X_4)$.

b) product of two tensors $\boldsymbol{X}:\boldsymbol{Y}$ (tensor with *ijkl* components equal to $X_{ijmn}Y_{mnkl}$) is

$$\begin{aligned} \mathbf{X}:\mathbf{Y} = &(2X_1Y_1 + X_3Y_4)\mathbf{T}^{(1)} + X_2Y_2\mathbf{T}^{(2)} + (2X_1Y_3 + X_3Y_6)\mathbf{T}^{(3)} \\ &+(2X_4Y_1 + X_6Y_4)\mathbf{T}^{(4)} + \frac{1}{2}X_5Y_5\mathbf{T}^{(5)} + (X_6Y_6 + 2X_4Y_3)\mathbf{T}^{(6)} \end{aligned} \tag{A.5}$$

If x_3 is the axis of transverse symmetry, general transversely isotropic fourth-rank tensor, being represented in this basis

$$\Psi_{ijkl} = \sum \psi_m T^m_{ijkl}$$

has the following components:

$$\psi_1 = (\Psi_{1111} + \Psi_{1122})/2; \quad \psi_2 = 2\Psi_{1212}; \quad \psi_3 = \Psi_{1133}; \quad \psi_4 = \Psi_{3311};$$
$$\psi_5 = 4\Psi_{1313}; \quad \psi_6 = \Psi_{3333} \tag{A.6}$$

In particular:

- Tensor of elastic compliances of the isotropic material $S_{ijkl} = \sum s_m T^m_{ijkl}$ has the following components

$$s_1 = \frac{1-\nu}{4G(1+\nu)}; \quad s_2 = \frac{1}{2G}; \quad s_3 = s_4 = \frac{-\nu}{2G(1+\nu)}; \quad s_5 = \frac{1}{G}; \quad s_6 = \frac{1}{2G(1+\nu)} \tag{A.7}$$

- Tensor of elastic stiffness of the isotropic material by $C_{ijkl} = \sum c_m T^m_{ijkl}$ has components

$$c_1 = \lambda + G; \quad c_2 = 2G; \quad c_3 = c_4 = \lambda; \quad c_5 = 4G; \quad c_6 = \lambda + 2G \tag{A.8}$$

Where $\lambda = 2G\nu/(1-2\nu)$.

- Components of fourth-rank Hill's tensor for elasticity problem $\hat{\mathbf{Q}}^{\Omega}$ are:

$$q_1 = G_0[4\kappa - 1 - 2(3\kappa - 1)f_0 - 2\kappa f_1], \quad q_2 = 2G_0[1 - (2-\kappa)f_0 - \kappa f_1]$$
$$q_3 = q_4 = 2G_0[(2\kappa - 1)f_0 + 2\kappa f_1], \quad q_5 = 4G_0(f_0 + 4\kappa f_1),$$
$$q_6 = 8G_0(\kappa f_0 - \kappa f_1) \tag{A.9}$$

$$f_0 = \frac{\gamma^2(1-g)}{2\left(\gamma^2-1\right)}; \quad g(\gamma) = \begin{cases} \frac{1}{\gamma\sqrt{1-\gamma^2}}\arctan\frac{\sqrt{1-\gamma^2}}{\gamma}, & \text{oblateshape } (\gamma > 1) \\ \frac{1}{2\gamma\sqrt{\gamma^2-1}}\ln\frac{\gamma+\sqrt{\gamma^2-1}}{\gamma-\sqrt{\gamma^2-1}}, & \text{prolateshape } (\gamma < 1) \end{cases} \tag{A.10}$$

For a thin (strongly oblate) spheroid ($a_1 = a_2 = a, \quad \gamma \equiv a/a_3 >> 1$): $g(\gamma) \to \frac{\pi}{2\gamma}, \quad f_0 \to \frac{\pi}{4}\gamma$

$$f_1 = \frac{\gamma^2}{4\left(\gamma^2-1\right)^2}\left[\left(2\gamma^2+1\right)g - 3\right], \quad \kappa = 1/[2(1-\nu_0)] \tag{A.11}$$

- Second rank Hill's tensor (Hill's tensor for conductivity problem) $\mathbf{Q}^{\Omega}$:

$$Q^{\Omega}_{ij} = k_0\left[(1 - f_0(\gamma))\delta_{ij} + (1 - 3f_0(\gamma))n_i n_j\right] \tag{A.12}$$

- Expressions for w_1, w_2, w_3 and w_4 that used in the formulas of (2.9) are:

$$\begin{aligned} w_1 &= \frac{1}{2} + \left[G_0\left(S^1_{1111} + S^1_{1122}\right) - \frac{1-\nu_0}{2(1+\nu_0)}\right][4\kappa - 1 - 2(3\kappa-1)f_0 - 2\kappa f_1] \\ &\quad + 2\left[G_0 S^1_{1133} + \frac{\nu_0}{2(1+\nu_0)}\right][(2\kappa-1)f_0 + 2\kappa f_1] \\ w_2 &= 1 + 8\kappa\left[G_0 S^1_{3333} - \frac{1}{2(1+\nu_0)}\right][f_0 - f_1] \\ &\quad + 4\left[G_0 S^1_{3311} + \frac{\nu_0}{2(1+\nu_0)}\right][(2\kappa-1)f_0 + 2\kappa f_1] \\ w_3 &= 2\left[G_0\left(S^1_{1111} + S^1_{1122}\right) - \frac{1-\nu_0}{2(1+\nu_0)}\right][(2\kappa-1)f_0 + 2\kappa f_1] \\ &\quad + 8\kappa\left[G_0 S^1_{1133} + \frac{\nu_0}{2(1+\nu_0)}\right][f_0 - f_1] \\ w_4 &= 2\left[G_0 S^1_{1133} + \frac{\nu_0}{2(1+\nu_0)}\right][4\kappa - 1 - 2(3\kappa-1)f_0 - 2\kappa f_1] \\ &\quad + 2\left[G_0 S^1_{3333} - \frac{1}{2(1+\nu_0)}\right][(2\kappa-1)f_0 + 2\kappa f_1] \end{aligned} \tag{A.13}$$

References

Anisimova, M., Knyazeva, A., & Sevostianov, I. (2016). Effective thermal properties of an aluminum matrix composite with coated diamond inhomogeneities. *International Journal of Engineering Science, 106*, 142–154.

Benveniste, Y. (1987). A new approach to the application of Mori-Tanaka's theory in composite materials. *Mechanics of Materials, 6*(2), 147–157.

Boden, A. (2015). *Copper graphite composite Materials: A novel way to engineer thermal conductivity and expansion*. Berlin: Freie Universität Berlin (Doctoral dissertation)Diss., 2015.

Bosak, A., Krisch, M., Mohr, M., Maultzsch, J., & Thomsen, C. (2007). Elasticity of single-crystalline graphite: Inelastic x-ray scattering study. *Physical Review B, 75*(15), 153408.

Chen, C. H., & Wang, Y. C. (1996). Effective thermal conductivity of misoriented short-fiber reinforced thermoplastics. *Mechanics of Materials, 23*(3), 217–228.

Chen, T. (1993). Thermoelastic properties and conductivity of composites reinforced by spherically anisotropic particles. *Mechanics of Materials, 14*(4), 257–268.

Chou, T. W., & Nomura, S. (1981). Fibre orientation effects on the thermoelastic properties of short-fibre composites. *Fibre Science and Technology, 14*(4), 279–291.

Ferrari, M., & Johnson, G. C. (1989). Effective elasticities of short-fiber composites with arbitrary orientation distribution. *Mechanics of Materials, 8*(1), 67–73.

Firkowska, I., Boden, A., Boerner, B., & Reich, S. (2015). The origin of high thermal conductivity and ultralow thermal expansion in copper–graphite composites. *Nano Letters, 15*(7), 4745–4751.

Horii, H., & Nemat-Nasser, S. (1983). Overall moduli of solids with microcracks: Load-induced anisotropy. *Journal of the Mechanics and Physics of Solids, 31*(2), 155–171.

Kachanov, M., & Sevostianov, I. (2005). On quantitative characterization of microstructures and effective properties. *International Journal of Solids and Structures, 42*(2), 309–336.

Kachanov, M., Tsukrov, I., & Shafiro, B. (1994). Effective properties of solids with randomly located defects. In D. Breusse (Ed.), *Probabilities and Materials: Tests, Models and Applications* (pp. 225–240). Kluwer Publ.

Kanaun, S. K., & Levin, V. (2007). *Self-consistent methods for composites: Vol. 1: Static problems*: Vol. 148. Springer Science & Business Media.

Kováčik, J., Emmer, Š., & Bielek, J. (2016). Cross-property connections for copper–graphite composites. *Acta Mechanica, 227*(1), 105–112.

Kunin, I. A. (1983). Elastic medium with random fields of inhomogeneities. In *Elastic media with microstructure II* (pp. 165–228). Berlin, Heidelberg: Springer.

Kushch, V. I., & Sevostianov, I. (2016). Maxwell homogenization scheme as a rigorous method of micromechanics: Application to effective conductivity of a composite with spheroidal particles. *International Journal of Engineering Science, 98*, 36–50.

Ledbetter, H. M., & Naimon, E. R. (1974). Elastic properties of metals and alloys. II. Copper. *Journal of Physical and Chemical Reference Data, 3*(4), 897–935.

Lu, Y., & Liaw, P. K. (1995). Effects of particle orientation in silicon carbide particulate reinforced aluminum matrix composite extrusions on ultrasonic velocity measurement. *Journal of Composite Materials, 29*(8), 1096–1116.

Markov, K. Z. (2000). Elementary micromechanics of heterogeneous media. In *Heterogeneous media* (pp. 1–162). Boston: Birkhäuser.

Marzari, N., & Ferrari, M. (1992). Textural and micromorphological effects on the overall elastic response of macroscopically anisotropic composites. *Journal of Applied Mechanics, 59*(2), 269–275.

Maxwell, J. C. (1873). *A treatise on electricity and magnetism*. Clarendon Press.

Mazloum, A., Kováčik, J., Emmer, Š., & Sevostianov, I. (2016). Copper–graphite composites: Thermal expansion, thermal and electrical conductivities, and cross-property connections. *Journal of Materials Science, 51*(17), 7977–7990.

Nelson, J. B., & Riley, D. P. (1945). The thermal expansion of graphite from 15 c. to 800 c.: Part I. Experimental. *Proceedings of the Physical Society, 57*(6), 477.

Pettermann, H. E., Böhm, H. J., & Rammerstorfer, F. G. (1997). Some direction-dependent properties of matrix-inclusion type composites with given reinforcement orientation distributions. *Composites Part B: Engineering, 28*(3), 253–265.

Sevostianov, I. (2012). On the thermal expansion of composite materials and cross-property connection between thermal expansion and thermal conductivity. *Mechanics of Materials, 45*, 20–33.

Sevostianov, I. (2014). On the shape of effective inclusion in the Maxwell homogenization scheme for anisotropic elastic composites. *Mechanics of Materials, 75*, 45–59.

Sevostianov, I., & Giraud, A. (2013). Generalization of Maxwell homogenization scheme for elastic material containing inhomogeneities of diverse shape. *International Journal of Engineering Science, 64*, 23–36.

Sevostianov, I., & Kachanov, M. (1999). Compliance tensors of ellipsoidal inclusions. *International Journal of Fracture, 96*(1), 3–7.

Sevostianov, I., & Kachanov, M. (2002). Explicit cross-property correlations for anisotropic two-phase composite materials. *Journal of the Mechanics and Physics of Solids, 50*(2), 253–282.

Sevostianov, I., & Kachanov, M. (2009). Connections between elastic and conductive properties of heterogeneous materials. *Advances in Applied Mechanics, 42*, 69–252.

Takao, Y., Chou, T. W., & Taya, M. (1982). Effective longitudinal Young's modulus of misoriented short fiber composites. *Journal of Applied Mechanics, 49*(3), 536–540.

Tong, X. C. (2011). *Advanced materials for thermal management of electronic packaging*: Vol. 30. Springer Science & Business Media.